

KAWASAKI STEEL TECHNICAL REPORT

No.22 (May 1990)

*Advanced Technologies of Iron and Steel,
Commemorating the 20th Anniversary
of the Technical Research Division*

Energy Dispersive Full-Automatic Texture Analyzer

Tizuko Maeda, Michio Katayama, Masato Shimizu

Synopsis :

Energy dispersive full-automatic texture analyzer has newly been developed using Mo white X-ray diffraction. Pole figures of (110), (200) and (211) of α -Fe can be analyzed from respective integral peak intensities measured at the same time with the Ge detector system set up at 14° from incident X-ray beams, after escape peak correction. Measuring time of a complete pole figure is about 200 min, which is 40 min longer than that of conventional angular dispersive texture analyzers, but that of three kinds of complete pole figures for obtaining an orientation distribution function is less than half the time by conventional texture analyzers.

(c)JFE Steel Corporation, 2003

The body can be viewed from the next page.

Energy Dispersive Full-Automatic Texture Analyzer*



Tizuko Maeda
Researcher,
Instrumentation &
Analytical Science
Research Center



Michio Katayama
Senior Researcher,
Instrumentation &
Analytical Science
Research Center



Masato Shimizu
Dr. Engi., Senior
Researcher,
Instrumentation &
Analytical Science
Research Center

Synopsis:

Energy dispersive full-automatic texture analyzer has newly been developed using Mo white X-ray diffraction. Pole figures of (110), (200) and (211) of α -Fe can be analyzed from respective integral peak intensities measured at the same time with the Ge detector system set up at 14° from incident X-ray beams, after escape peak correction. Measuring time of a complete pole figure is about 200 min, which is 40 min longer than that of conventional angular dispersive texture analyzers, but that of three kinds of complete pole figures for obtaining an orientation distribution function is less than half the time by conventional texture analyzers.

1 Introduction

With the development of high power X-ray tubes and improvement in the energy resolution of solid state detectors (SSD) and preamplifiers, the energy dispersive X-ray diffraction (EDXD) technique is now often applied to the structural study of materials. One of the most substantial benefits of the EDXD technique is its ability to measure the X-ray diffraction pattern at a fixed reflection geometry. An energy dispersive inverse pole figure analyzer was previously developed by setting up a planar intrinsic Ge detector on a Bragg-Brentano parafocusing goniometer.¹⁾ Subsequently, the inverse pole figures of up to 200 specimens have been measured fully automatically at one measurement chance. In addition, the EDXD technique offers great advantages over the conventional angular dispersive X-ray diffraction (ADX) technique²⁾, since several types of pole figures can be measured simultaneously using the white X-ray energy spectrum, resulting in a substantial saving in time in the determination of the orientation distribution function (ODF).

This paper reports on a fully automatic energy dispersive texture analyzer newly developed in cooperation with Rigaku Corporation.

2 Principles and Characteristics of Pole Figure Measurement by EDXD Technique

In anisotropic polycrystalline metallic materials, such

as grain-oriented silicon steel and deep drawable cold-rolled steel, texture analysis on a large scale is indispensable for the improvement of properties and quality control of final products.

The principal objects of the development were as follows:

- (1) To reduce the time required to determine ODF by making possible simultaneous recording of several types of pole figures using the EDXD technique
- (2) To establish a method of data processing and correction in EDXD measurement
- (3) To realize a fully automatic system for incomplete pole figure measurement covering operations from sample changing to figure drawing

The principles and characteristics of pole figure measurement by the EDXD technique should be reviewed briefly before the specifications of new texture analyzer are presented.

The pole figure is a diagram of a pole density function of the (hkl) plane normal produced by the stereographic projection. It depicts the direction of the preferred orientation of a polycrystalline sample. The pole density function is a normalized variation of diffraction X-ray intensities, which are in general obtained with a counter diffractometer by the ADXD technique. The counter is fixed at the diffraction angle $2\theta_{hkl}$ given by the Bragg's equation (Eq. (1)) for the chosen (hkl) plane, and the specimen is rotated about two perpendicular axes, as discussed later, so as to permit the measurement of the integrated intensities diffracted by the selected planes oriented at various angles within the specimen.

* Originally published in *Kawasaki Steel Giho*, 21(1989)2, pp. 88-92

$$2d_{hkl} \sin \theta_{hkl} = \lambda_0 \dots \dots \dots (1)$$

where λ_0 : Wavelength of the characteristic X-ray
 d_{hkl} : Interplanar spacing between the (hkl) lattice planes

With this method, only one type of pole figure can be measured for the selected geometry, because the Bragg's angle θ_{hkl} changes with respect to the d -value. For this reason, the analysis of the quantitative ODF calculated from several types of pole density functions is exceedingly time-consuming.

In contrast, the Bragg's equation in the EDXD technique is as follows:

$$E_{hkl} = hc/\lambda_{hkl} = 6.2/(d_{hkl} \sin \theta) \dots \dots \dots (2)$$

where E_{hkl} is diffracted X-ray photon energy for the chosen (hkl) plane and θ is a suitable setting angle of the incident X-ray beam and (hkl) plane. Diffraction peaks can be recorded simultaneously at the fixed setting angle. The solid lines in Fig. 1 show the setting angle dependences of the diffraction X-ray photon energy of α -Fe calculated by Eq. (2). The diffraction X-ray photon energy increases as the incident angle decreases and as the Miller indices (hkl) of the diffraction planes become greater. In the present measurement, (110), (200) and (211) peaks corresponding approximately to 25 keV, 35.5 keV and 43.5 keV respectively on a diffraction spectrum are simultaneously recorded at a setting angle of 7° .

It should be noted that in EDXD measurement, escape peaks from the SSD, Compton scattering intensity, and the contribution of the white X-ray energy distribution of the incident beam must be eliminated from the diffraction energy spectrum.³⁾ When X-ray photons with higher energy than the K-absorption edge of Ge penetrate into the intrinsic region, which is composed of a very pure Ge single crystal, Ge $K\alpha$ radiation is

emitted as in excitation and escapes from the diode, and therefore escape peaks appear on the diffraction spectrum at lower Ge $K\alpha$ radiation energies (9.87 keV) than those of the Bragg peaks. Since the intensities of the escape peaks are determined by the escape yield relative to penetrating X-ray photons, their values depend on the intensity of the diffraction X-ray.

The necessary information for pole figure analysis is the distribution of Bragg peak intensities at a characteristic energy. Therefore, white X-ray energy distribution and Compton scattering intensities, which are independent of diffraction X-ray intensities, are eliminated by analysis of the pole density function, while escape peak correction is required when the escape peak overlaps with the Bragg peak, because of the dependence of the escape peak on the peak intensity of the diffraction X-ray, as mentioned above.

The dotted lines in Fig. 1 show the setting angle dependences of the X-ray photon energies of escape peaks which appear at respective Bragg peaks of α -Fe. In general, (110), (200) and (211) pole figures are adopted for the precise ODF analysis of α -Fe, but all setting angles have the overlap shown in Fig. 1. For this reason, escape peak correction in the new texture analyzer is performed as follows: Energy of the escape peak caused by the (200) diffraction peak is set closely over the energy of the (110) diffraction peak by use of a setting angle of 7° , and the intensity of the escape peak is thus eliminated from the (110) peak intensity. The escape peak intensity, which shows the characteristic X-ray energy dependence of the SSD, can be obtained by multiplying the (200) peak intensity by the escape yield given by a suitable standard sample, such as a Si single crystal.³⁾

This correction is not necessary, however, for the pole figure measurement of γ -Fe, because of the absence of an overlap at the setting angle of 7° .

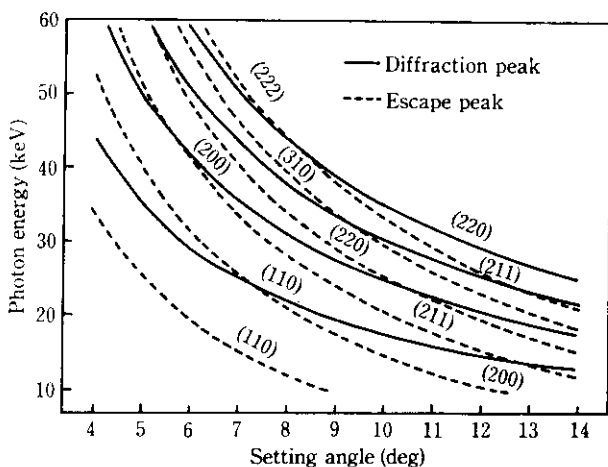


Fig. 1 Incident angle dependences of energy of diffraction X-ray peaks of α -Fe and escape X-ray peaks by SSD

3 System Diagram and Specifications of New Texture Analyzer

The appearance, system diagram, and principal specifications of the new device are shown in Photo 1, Fig. 2 and Table 1, respectively.

3.1 X-Ray Optical System

The X-ray source is a Rigaku RU-300 rotating anode X-ray generator with an Mo target of maximum 60 kV and 300 mA.

The goniometers for complete and incomplete pole figures are symmetrically arranged on the right and left side of the device, as shown in Photo 1, and can be separately operated. Both are normal pole figure goniometers with two perpendicular rotation axes, α (rotation about RD) and β (rotation about ND), and a vibration axis γ perpendicular to them, and are arranged for the Schulz geometry shown in Fig. 3.

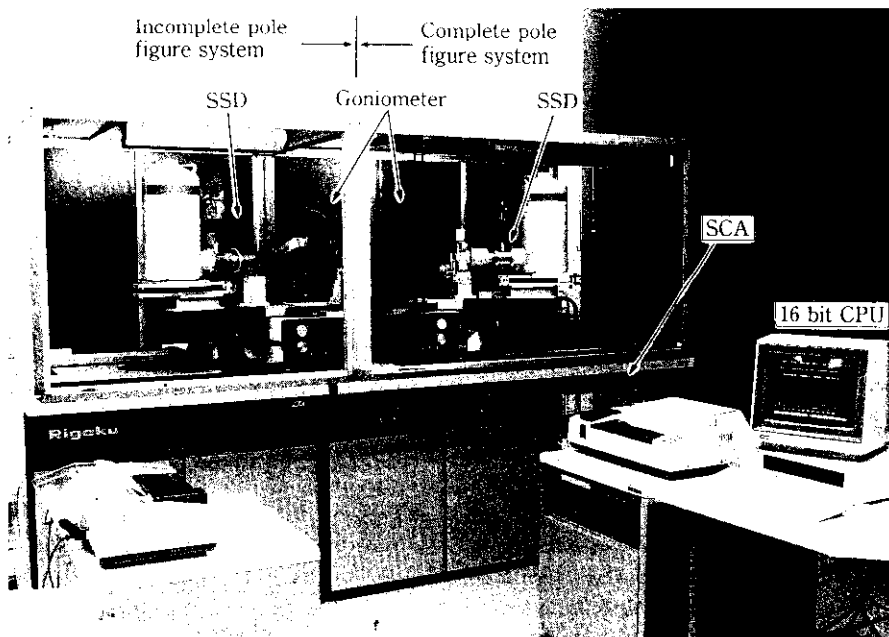


Photo 1 Energy dispersive full-automatic texture analyzer

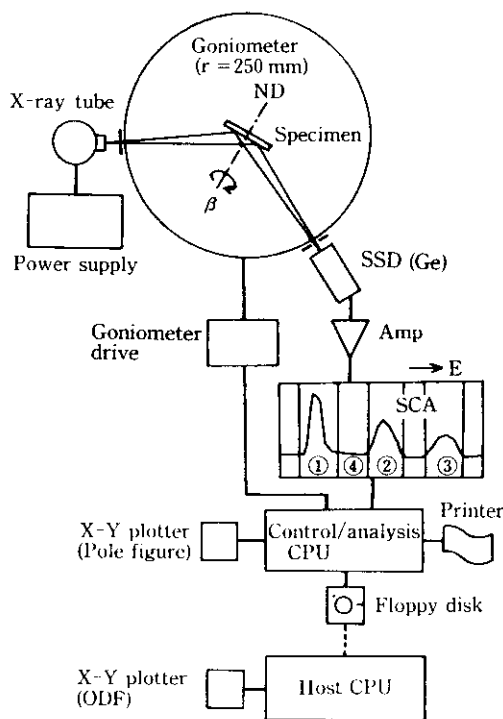


Fig. 2 System diagram

The incomplete pole figure is measured by reflection geometry for α from 10° to 90° . The outer region for α values from 0° to 10° cannot be determined reliably because of defocussing and loss of intensity. On the other hand, a complete pole figure is measured by

Table 1 Specifications

	Complete pole figure	Incomplete pole figure
X-ray tube	Mo (white X-ray)	
Target	≤ 60 kV, 300 mA (max 18 kW)	
Power	0.5 mm \times 10 mm	
Focus		
Goniometer	$r=250$ mm (Schulz geometry)	$r=250$ mm (Schulz geometry)
α -scanning	$0-40^\circ$ (trans.) $30-90^\circ$ (ref.)	$10-90^\circ$ (ref.)
β -scanning	$0-360^\circ$ (trans./ref.)	$0-360^\circ$ (ref.)
Detector	Ge SSD	Ge SSD
Energy analyzer	SCA \times 4	SCA \times 4
Count meter	Dual counter	Dual counter

transmission geometry for α from 0° to 40° and by reflection geometry in the range from 30° to 90° , and intensity data from the overlap region from 30° to 40° is used to establish a common basis for the transmission and reflection intensities. The rotation steps in an incomplete pole figure measurement are $\Delta\alpha = 10^\circ$ and $\Delta\beta = 5^\circ$; in a complete pole figure measurement for precise ODF analysis, the steps are $\Delta\alpha = \Delta\beta = 5^\circ$. The methods of specimen scanning for complete and incomplete pole figure measurements are the same as in conventional ADXD measurement.²⁾

An automatic sample-changer capable of setting up to 12 specimen sheets is installed with the incomplete

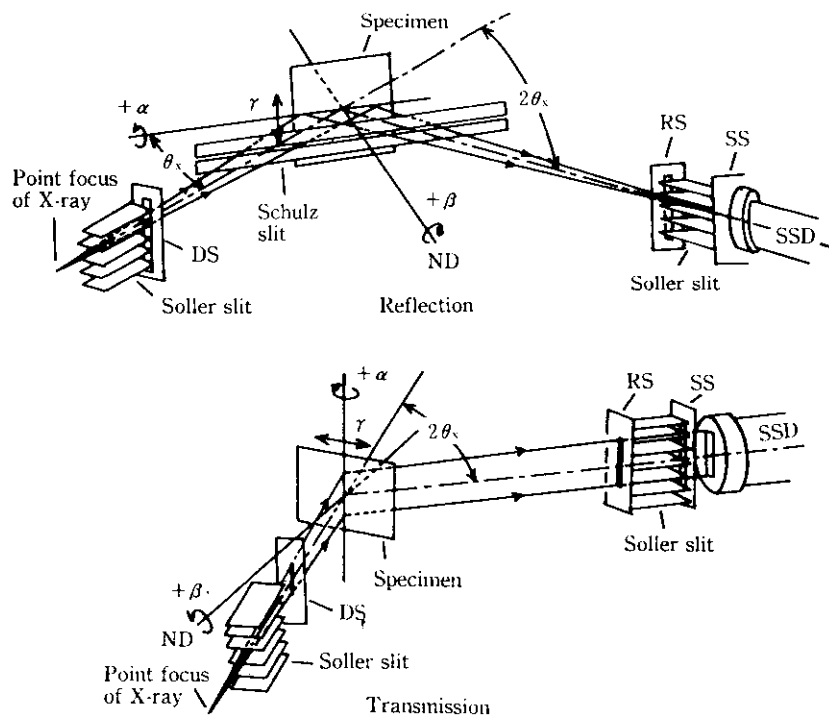


Fig. 3 Reflection and transmission geometries

pole-figure goniometer, permitting fully automatic all-night operation.

3.2 X-Ray Detection System

Diffraction X-ray photons are detected by an intrinsic Ge SSD with high quantum efficiency for 10~50 keV. The energy pulses transmitted through the preamplifier and pulse shaping amplifier are stored in four single-channel analyzers (SCA 1-4).

Figure 4 is a diffraction spectrum of α -Fe at a setting

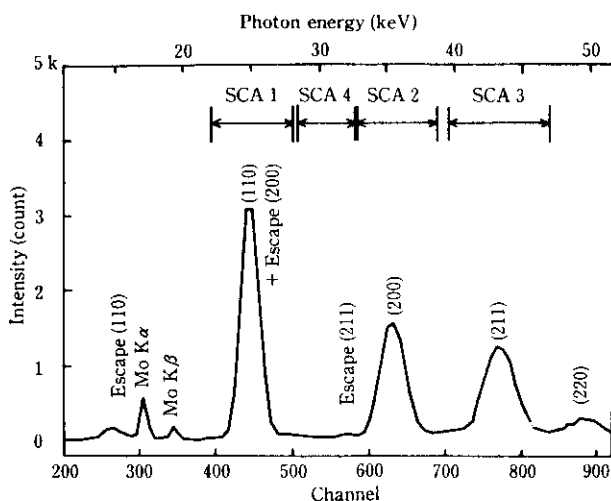


Fig. 4 Diffraction spectrum of α -Fe by energy dispersive technique at $\theta = 7$ deg

angle of 7° . Bragg peaks, (110), (200) and (211) and the background between the (110) peak and (200) peak are analyzed by SCA 1, 2, 3 and 4, respectively, as shown in Fig. 4. Backgrounds of respective Bragg peaks are simply determined by multiplying the background intensity of SCA 4 by the respective ratios of the energy windows of the Bragg peaks to the background, and are then eliminated from the peak intensities of SCA 1-3. Further, the intensity of the escape peak caused by the (200) peak is eliminated from the intensity of the (110) peak.

3.3 System Control and Data Processing

System operation control and data processing are performed respectively by two 16-bit personal computers connected in parallel with the two pole figure devices.

First, it is necessary to input the conditions for system operation and subsequent data processing, such as the step widths of α and β rotations, the fixed time per rotation step, the energy window ratios for determination of the backgrounds of the respective Bragg peaks, the escape yield, and the μt -value. Here, μ and t are the linear absorption coefficient and the thickness of the specimen respectively. Next, measurement begins after data files for (110), (200) and (211) pole figures are recorded on a floppy disk. After the background and the escape peak are eliminated from the integrated intensities stored in SCA 1-3 step by step, the Bragg peak intensities are memorized in the file. Variations in diffraction intensity in the β rotation cycle can be moni-

tored for each step of the α rotation.

On completion of the incomplete pole figure measurement of the first specimen, measurement of the next specimen proceeds in the same manner. Data analysis and incomplete pole figure drawing are carried out during the measurement of the next specimen. Incomplete pole figure measurements of up to 12 specimens can be performed fully automatically.

Complete pole figures are measured one by one, because individual specimens have different μt -values; this measurement is much more time-consuming than incomplete pole figure measurement. Before diffraction measurement, the precise measurement of the μt -value is performed as follows: The specimen is set vertically relative to the incident beam immediately in front of the receiving slit, and the diminution in intensity of a monochromatic beam of X-rays passing perpendicularly through the specimen is determined. Based on the degree of diminution, (I_m/I_0) , a μt -value is obtained, as shown in Eq. (3).

$$\mu t = -\ln(I_m/I_0) \dots\dots\dots(3)$$

where, I_0 and I_m are the original and transmission monochromatic beam intensities, respectively. The monochromatic beam used is a diffraction X-ray from a suitable sample.

The pole density function is the normalized distribution of the relative intensity ratio of a specimen to that of a randomly oriented standard specimen with the same material components, and this is similar to that in the conventional ADXD method.²⁾ In the new texture analyzer, however, the pole density function can also be determined by absorption correction formula.⁴⁾

The orientation distribution function given by Roe's Euler angles⁵⁾ is calculated from three types of pole density functions, (110), (200) and (211) with a host

computer.

4 Complete Pole Figure of Cold-Rolled Steel Sheet

Figure 5 shows (110), (200) and (211) complete pole figures of a cold-rolled steel sheet as measured by the new texture analyzer. Figure 6 shows the ODF section for $\phi = 45^\circ$ calculated from Fig. 5. It is evident that a typical cold-rolling texture with $\{111\} \langle 112 \rangle$ orientation is formed and that the main components are $(\bar{1}11)$ $[1\bar{1}2]$ and $(\bar{1}11)$ $[12\bar{1}]$.

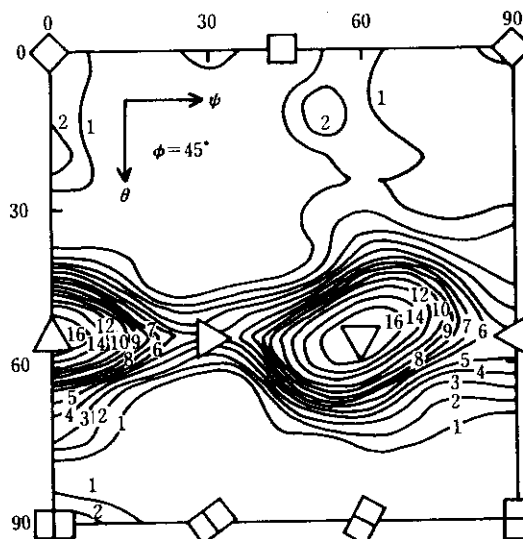


Fig. 6 Crystallite orientation distribution function (ODF) calculated from (110), (200) and (211) pole figures of Fig. 5

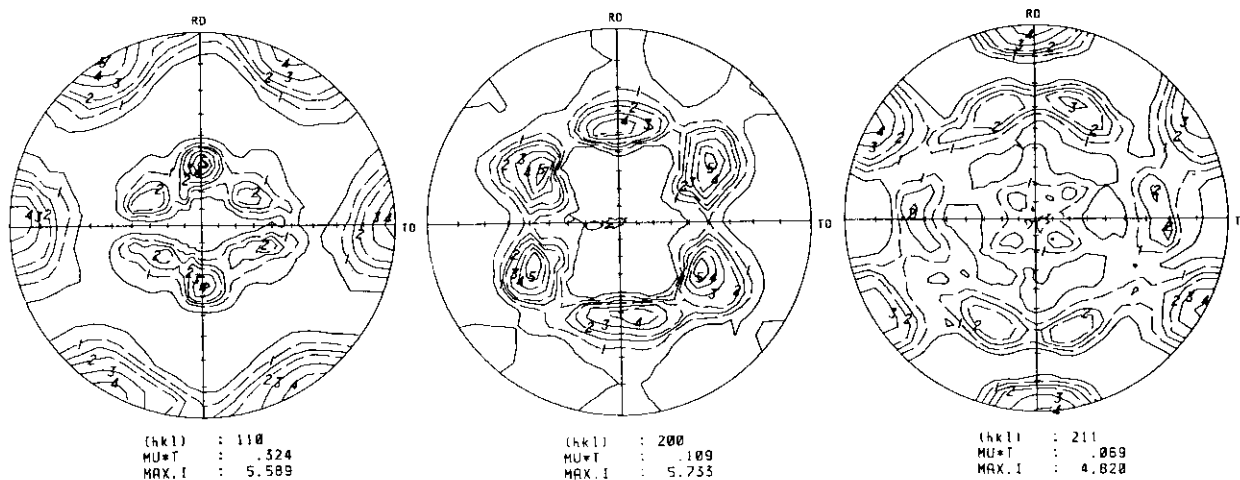


Fig. 5 Complete pole figures of cold rolled steel sheet by newly developed system at $\theta = 7$ deg (MU (μ), absorption coefficient; T, thickness of specimen)

5 Comparison of Measurement Time

A comparison of the measurement times of the two techniques, EDXD and ADXD, under conditions giving similar results is presented below.

The measurement of an incomplete pole figure with the new device requires about 70 min, which is almost equal to that with the conventional device. Total detection time is 44 min ($4 \text{ s/step} \times 648 \text{ steps}$), the same as with the conventional device, while the remainder, including goniometer scanning time, is 25 min. However, up to 12 specimens can be measured over night using the automatic sample changer.

On the other hand, the measurement of a complete pole figure with the new device requires 208 min, which is 40 min longer than the 168 min with the conventional device. This increase in measurement time is due to the increase in the total detection time for X-rays, since the fixed time in a reflection region with 936 steps is 8 s, or 2 times as long as the conventional fixed time of 4 s (although the fixed time in a transmission region with 648 steps is 2 s). Since the diffraction X-ray energies by EDXD are higher than the $\text{MoK}\alpha$ (17.44 keV) in the conventional ADXD method, and linear absorption coefficients are $1/13 \sim 1/15$ the value in ADXD, X-ray intensities in the reflection region are weaker than those in the transmission region. For this reason, the measurement time in the reflection region is prolonged.

However, since three types of complete pole figures can be measured simultaneously, the ODF measurement can be performed in less than $1/2$ the time required for ADXD.

6 Conclusions

- (1) A fully automatic energy dispersive texture analyzer was newly developed. The device uses Mo white X-ray diffraction and makes possible simultaneous measurement of pole figures.
- (2) Pole figures of (110), (200) and (211) of α -Fe can be analyzed from respective integrated peak intensities stored simultaneously by the intrinsic Ge detector system at a setting angle of 7° , after escape peak correction. In contrast, pole figures of γ -Fe can be measured without escape peak correction using the same reflection geometry.
- (3) Measurement time for an incomplete pole figure is about 70 min, the same as that with a conventional device; that of a complete pole figure is about 200 min, which is longer than that with a conventional device. However, ODF measurement can be performed in less than half the time required for ADXD.

References

- 1) M. Katayama, M. Shimizu, M. Konishi, H. Kitagawa, and K. Morimoto: *Tetsu-to-Hagané*, **70**(1984)5, S564.
- 2) H. Kitagawa, M. Katayama, K. Morimoto, H. Maruyama, and K. Tsuruoka: *Tetsu-to-Hagané*, **63**(1977)1, 147-153.
- 3) T. Yamanaka: *Nippon-Kessho-Gakkaishi (J. Cryst. Soc. Japan)*, **30**(1988)4, 245-253.
- 4) S. Nagashima: "Shugo-Soshiki (Texture)", (1984), 9, [Maruzen].
- 5) R. J. Roe: *J. Appl. Phys.*, **36**(1965)6, 2024-2031.